

# Simulating the Effects of Projectile Explosion on a Jointed Rock Mass Using 2D DEM: A Case Study of Ardebil-Mianeh Railway Tunnel

H. Shahnazari<sup>1</sup>, M. Esmaili<sup>2</sup> and H. Hosseini Ranjbar<sup>3</sup>

Received: June 2009

Accepted: March 2010

**Abstract:** Considerations on the explosion resistant design of special infrastructures have increased in the recent years. Amongst the various types of infrastructures, road and railway tunnels have a unique importance due to their vital role in connection routes in emergency conditions. In this study, the explosion effects of a projectile impacting on a railway tunnel located in a jointed rock medium has been simulated using 2D DEM code. Primarily, a GP2000 projectile has been considered as a usual projectile and its penetration depth plus its crater diameter were calculated in rock mass. The blast pressure was, then, calculated via empirical formula and applied on the boundary of crater as input load. Finally, the wave pressure propagation through the jointed rock medium was investigated. In part of the study a sensitivity analysis has been carried out on jointed rock parameters such as joint orientation, dynamic modulus and damping ratio. Their effects on tunnel lining axial force as well as bending moment have also been investigated.

**Keywords:** Jointed rock medium, Projectile, Blast pressure, DEM

## 1. Introduction

Underground structures have been an active topic of world concern from a defensive point of view throughout the recent years. Amongst such structures, road and railway tunnels acting as transportation routes have been an important liability as blast resistant structures. Thus, the tunnel surrounding medium may act as an efficient means of defending against possible attacks. Rock masses due to their various forms of discontinuities such as cracks, joints, faults, bedding planes and etc, have shown a complex behavior. The presence of discontinuities in rock masses has a great influence on reflecting and attenuating the shock wave induced by projectile explosion. Modeling the blast phenomenon in jointed rock either numerically or experimentally have become the well known methods in the past decades. The experimental studies including a

combination of the structure elements, rock and loadings, are scarce as the full-scale experiments are expensive and model tests seem to be unrealistic, in particular, in replicating the self-weight of overburden rock [1].

Numerical simulation is relatively affordable and is becoming more and more indispensable in engineering analysis and design. The use of numerical methods is essential in understanding of the complex response seen in some experiments prior to the developments of any design guidelines [1]. Ma et al. (1998) studied the propagation of blast wave in jointed rock masses due to underground explosion using UDEC [2]. Chen and Zhao (1998) used the AUTODYN and UDEC codes simultaneously to model the shock wave propagation in jointed rock media. Their results agreed with those obtained from experimental modeling [3]. Fan et al. (2004) pursued the study of stress-history input (SHI) and velocity-history input (VHI) on wave propagation and wave attenuation in jointed rock masses using the discrete element method (DEM) [4]. Morris et al. (2004) simulated the response of a large-scale facility including several tunnel sections to dynamic loading caused by an underground explosion, using the 3D discrete element code LDEC [5]. Lu (2005) investigated the effect of various parameters such as geological conditions, explosive density and the geometry of explosive opening, on blast

---

\* Corresponding author: Email: hshahnazari@iust.ac.ir

1 Assistant Professor, School of Civil Engineering, Iran University of Science and Technology, Tehran, Iran.

2 Assistant Professor, School of Railway Engineering, Iran University of Science and Technology, Tehran, Iran.

3 Master's Degree graduate, School of Civil Engineering, Iran University of Science and Technology, Tehran, Iran.

phenomenon in a site in Sweden and modeled the results using artificial neural network [6]. Heuze and Morris (2006) carried out a series of experimental and field tests in order to model the blast effects in jointed rock media. They also made numerical modelings using LDEC. Comparing the DEM results to realistic outputs, they observed a considerable level of agreements between the two [7]. Jiao et al. (2007) applied a viscous boundary to Shi's DDA code in order to investigate its effect on wave propagation in jointed rock media [8]. Wang et al. (2008) studied wave propagation and the spalling caused by the phenomenon via numerical methods [9].

The main objective of the present paper is to study the stability of a railway tunnel lining against dynamic loading caused by a projectile explosion using the discrete element code, UDEC, when the tunnel is located in a jointed rock mass.

## 2. Ground Conditions at Ardebil – Mianeh Railway Tunnel

The third section of Ardebil-Mianeh Railway tunnel runs between STA 345+438 m and 345+558 m. It is located in the north of Ghezal Ozon River at North-West of Iran. The tunnel direction is N192 degrees and according to geological profiles the tunnel has a slope of -1.6%. The longitudinal geological section of the tunnel is given in Figure 1.

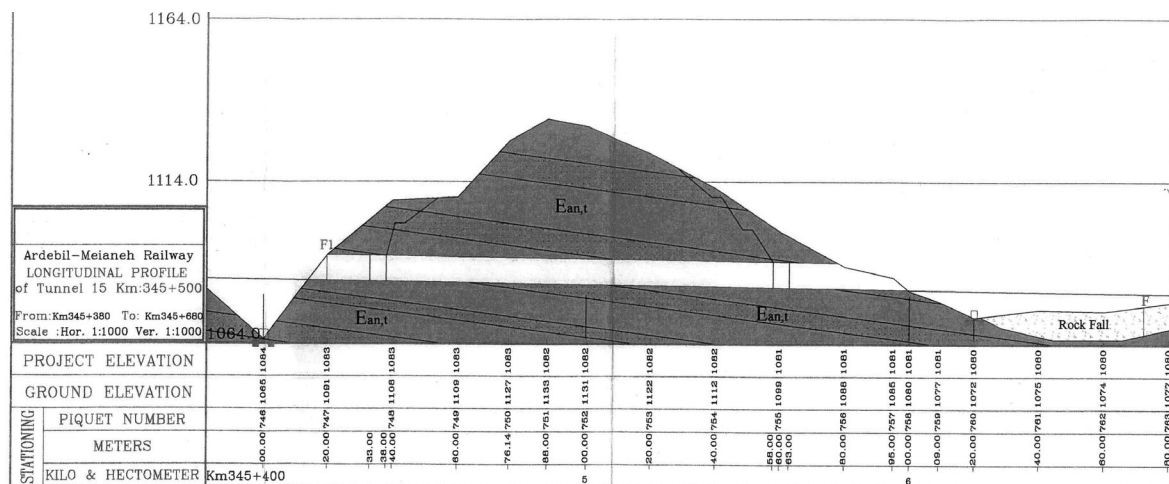


Fig. 1. The longitudinal geological section of Ardebil-Mianeh railway tunnel.

## 2.1. Geological conditions

The ground at section 3 of Ardebil-Mianeh tunnel consists, mainly, of andesite and agglomerate rocks. The ground water table is approximately 18 and 9 meters below the tunnel inlet at the portals. Thus, the effect of ground water is considered to be negligible.

## 2.2. Rock Mechanics data

The Schmidt Hammer Rebound test was carried out as a primary test in order to determine the uniaxial compressive strength and also the

Table 1. Intact rock data at Ardebil-Mianeh railway tunnel [10].

| Rock type   | Elastic modulus, E (GPa) | Cohesion, C (MPa) | Friction angle, $\Phi$ ( $^\circ$ ) | Compressive strength, $\sigma_{ci}$ (MPa) | Tensile strength (MPa) |
|-------------|--------------------------|-------------------|-------------------------------------|---|------------------------|
| Andesite    | 82                       | 10                | 46                                  | 160                                       | 20                     |
| Agglomerate | 38.4                     | 4.5               | 39.5                                | 48  | 6.5                    |

elastic moduli ( $E_i, \sigma_{ci}$ ). The test results along with other intact rock properties are given in Table 1.

## 2.3. Joint set data

According to the geological investigations, four major discontinuity sets are recognized throughout the tunnel length. The joint data obtained for section 3 of the Ardebil-Mianeh railway tunnel are presented in Table 2.

In accordance to the joint study, the Tilting test

**Table 2.** Joint data for section 3 of Ardebil-Mianeh railway tunnel [10].

| Joint set | dip/dip direction (°) | Spacing (m) | Filling (%)         | Moisture content |
|-----------|-----------------------|-------------|---------------------|------------------|
| J1        | 81/122                | 0.6         | 90 Empty<br>10 Soil | dry              |
| J2        | 84/328                | 0.7         | 90 Empty<br>10 Soil | dry              |
| J3        | 79/199                | 0.75        | 95 Empty<br>5 Soil  | dry              |
| Bedding   | 18/120                | -           | -                   | -                |

and the Schmidt Hammer Rebound test were carried out to determine the friction angle and compressive strength of joint sets.

The normal,  $K_n$ , and shear,  $K_s$ , Stiffness were calculated according to elastic formulae [11]:

$$K_n = \frac{E_m E_r}{s(E_r - E_m)} \quad \text{and} \quad K_s = \frac{G_m G_r}{s(G_r - G_m)} \quad (1)$$

Where  $E_m$  is the rock mass Young's modulus,  $E_r$  is the intact rock Young's modulus,  $G_m$  is the rock mass shear modulus,  $G_r$  is the intact rock shear modulus and  $s$  is the joint spacing. The rock mass elastic modulus was reported 14.2 and 4.15 GPa for andesite and agglomerate, respectively. However, in order to obtain conservative results, properties of weaker rock were used in calculations. The joint properties obtained for the

**Table 3.** Rock joint parameters obtained for section 3 of Ardebil-Mianeh railway tunnel [10].

| Joint property | Cohesion, C (MPa) | Friction angle, $\Phi$ (°) | Normal stiffness, $K_n$ (GPa) | Shear stiffness, $K_s$ (GPa) | Tensile strength (MPa) |
|----------------|-------------------|----------------------------|-------------------------------|------------------------------|------------------------|
|                | 0.2               | 35                         | 10                            | 4                            | 0.2                    |

Ardebil-Mianeh Railway tunnel are given in Table 3.

### 2.4. Dynamic rock properties

Estimating the rock's dynamic properties is usually a complicated process, due to the rock's complex behavior. However, amongst the dynamic properties, the dynamic Young's modulus has been studied to a greater extent. Hayashi (1973) suggested the following correlation between the rock's dynamic and static Young's modulus:

$$E_d = (1.3 - 1.7) E_s \quad (2)$$

## 3. Weapon Characteristics

In this study, the high-explosive general-purpose projectile (GP2000), which is used for general destruction by blast and fragmentation, was assumed. The general characteristics of GP2000 projectile are given in Table 4.

**Table 4.** General characteristics of GP2000 projectile [12].

| Property | Total weight | Charge-weight | Body diameter | Slenderness ratio | Striking velocity |
|----------|--------------|---------------|---------------|-------------------|-------------------|
| BS units | 2090 (lb)    | 1100 (lb)     | 23 in         | 3                 | 1100 (ft/sec)     |
| SI units | 950 (kg)     | 500 (kg)      | 585 mm        |                   | 335 (m/sec)       |

### 3.1. Projectile penetration depth

Due to the rock's complex behavior, projectile penetration is still under investigation throughout the world. A large range of theoretical and empirical knowledge regarding explosives and their effects has been developed from a series of researches and tests.

In this study, the empirical formula obtained by the U.S. Dept of Army [12] has been used as an initial estimate of penetration depth. According to the intact rock and projectile properties, a penetration depth of about 18 inches was derived which is unacceptable as it should be at least 3 times the projectile diameter. Young (1972) suggested the following formula for the penetration depth [13]:

$$P = 0.0031SN \left( \frac{W_p}{A} \right)^{0.5} (V - 100) \quad V \geq 200 \text{ ft/sec} \quad (3)$$

Where,

P = Depth of vertical penetration in feet,

$W_p$  = Total projectile weight in lb,

A = Cross-sectional area of the projectile in in<sup>2</sup>,

V = Striking velocity in feet/sec,

S = Constant for soil and rocks (equal to 1.07

for all rocks), and

N = Projectile nose shape factor.

**Table 5.** Validity range of Young's equation.

|               |                  |
|---------------|------------------|
| Weight (W)    | 2 to 3750 lb     |
| Diameter (in) | 1 to 30 in       |
| $W_p/A$       | 0.1 to 38 psi    |
| V             | 200 to 2370 fps. |

The validity range of Young's equation is given in Table 5.

Concerning projectile's properties, the Young's equation is valid for the GP2000 projectile. Substituting  $S = 1.07$ ,  $N = 1$  (for a tangent ogive nose shape) and replacing projectile's properties from Table 4, gives a penetration depth of 7.43 ft (2.26 m). On the other hand, according to the graphs given by Bangash (2009) a depth of 3.5 m is obtained. Thus, a value of 3 m is taken as penetration depth in the modeling process.

### 3.2. Crater size

A crater is defined as hole in the ground formed by an explosion [1]. Various factors such as the type and amount of explosive, projectile penetration depth, and the type of material in which the crater forms, control the final dimension of the crater [1]. However, no exact formulation has been derived for calculating the crater size.

According to graphs obtained by the U.S Dept of Army (1986), a large value was derived for the crater size, which is unacceptable from an engineering point of view.

Bangash (2009) proposed the following formula as an estimate for the crater radius [14]:

$$R_{vd} = \overline{K_{vd}^*} \sqrt[3]{W} \quad (4)$$

In which  $\overline{K_{vd}^*}$  is a coefficient depending on material type and  $W$  is the charge weight in kilograms. According to tables given in reference [1], a value of 0.15 is obtained for  $\overline{K_{vd}^*}$ .  $R_{vd}$  of about 1.1 m is thus derived. Referring to these values, a crater radius of 0.75 m was applied as an initial estimate in the current study.

### 3.3. Blast loading

A blast is usually modeled as a shock front which propagates from its source and attenuates as the distance from the explosion center increases. The blast loading may be characterized as a pulse with an exponential-shape time history that attenuates rapidly in amplitude and broadens as it propagates outward from the detonation center [1]. Thus, it is necessary to calculate the pressure-time history besides the peak pressure

value.

Estimating the peak overpressure due to a blast, based on the scaled distance ( $Z$ ), has been studied in a number of research works. The scaled distance is defined as:

$$Z = \frac{R}{W^{1/3}} \quad (5)$$

Where  $R$  is the distance from the center of explosion in meters and  $W$  is the equivalent charge weight in kilograms of TNT. Assuming that the explosive being used in GP2000 is Tritonal, the TNT equivalent weight is calculated to be:

$$W_{TNT} = W_{Tritonal} \times \frac{Q_{Tritonal}}{Q_{TNT}} = 500(\text{kg}) \times \frac{4932(\text{Kj/Kg})}{4520(\text{Kj/Kg})} = 545 \text{ Kg}$$

Where  $Q$  is the mass specific energy.

Thus,  $Z$  is derived to be  $0.092 \text{ mkg}^{-1/3}$  from equation 5. Accordingly, various peak pressure values have been worked out (based on formulae given in references [14] and [15]) and are given in Table 6.

To apply the appropriate value in our modeling process, several similar studies were also looked in: Gui and Chien (2006) derived a peak value of

**Table 6.** Various peak pressure values.

| Equation used             | Peak pressure value (Ps) |
|---------------------------|--------------------------|
| Nomienko (1956)           | 13.7 MPa                 |
| Newmark and Hansen (1961) | 800 MPa                  |
| Henrych (1979)            | 43.6 MPa                 |
| Mills (1987)              | 1.5 GPa                  |
| Brode (1995)              | 861 MPa                  |

20 MPa for soil [1]; Jiao et al. (2003) and Fan et al. (2004) implicated a value of 30 MPa in their modeling according to field results [4,8].

Finally, we applied the formula obtained by Henrych (1979) in our study [15]:

$$P_s = \frac{1407.2}{Z} + \frac{554.0}{Z^2} - \frac{35.7}{Z^3} + \frac{0.625}{Z^4} (\text{KPa})$$

$$0.05 \leq Z \leq 0.3$$

$$P_s = \frac{619.4}{Z} - \frac{32.6}{Z^2} + \frac{213.2}{Z^3} (\text{KPa})$$

$$0.3 \leq Z \leq 1 \quad (6)$$

$$P_s = \frac{66.2}{Z} + \frac{405}{Z^2} - \frac{328.8}{Z^3} (\text{KPa})$$

$$1 \leq Z \leq 10$$

Where  $Z$  is the scaled distance in  $mkg^{-1/3}$  and  $P_s$  is the peak overpressure. Henrych also derived the following equation for the blast duration:

$$\frac{t_a}{\sqrt[3]{W}} = 10^{-3}(0.107 + 0.444Z + 0.264Z^2 - 0.129Z^3 + 0.0335Z^4) \quad (7)$$

$0.05 \leq Z \leq 3$

Where  $t_a$  is the blast duration,  $W$  is the explosion charge weight in kg, and  $Z$  is the scaled distance. Inserting the  $Z$  and  $W$  values in equation 7, it gives the  $t_a = 1.22$  msec. According to the US Dept. of Army (1986), 10% of this time may be taken as the rise time ( $t_r$ ), i.e. the time required to reach  $P_s$ . Then after  $P_s$ , the shock wave decays monotonically according to equation (8) [12]:

$$P_t = P_0 e^{-t/t_a} \quad (8)$$

Where  $P_t$  is the blast pressure at any given time  $t$ . The resulting blasting pressure-time history curve applied to the crater inner boundary is shown in Figure 2.

#### 4. Numerical Modeling

The discrete element method (DEM) is suggested as an ideal alternative for modeling the joints in the rock mass and for their influence on the wave propagation [16]. UDEC is a 2D discrete element program specially designed to solve discontinuous problems in which the mechanical behavior of joints could be simulated under static and dynamic loading [17, 18].

In the modeling sequence, section containing the least overburden is considered as a critical

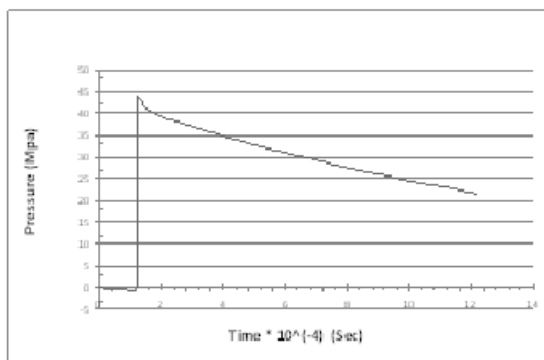


Fig. 2. Blasting pressure-time history curve applied to crater inner boundary.

section in relation to the blast effects caused by a projectile impact. According to longitudinal and transversal profiles, the section shown in Figure 3 which has an overburden about 12 m above the crown was chosen as the critical section.

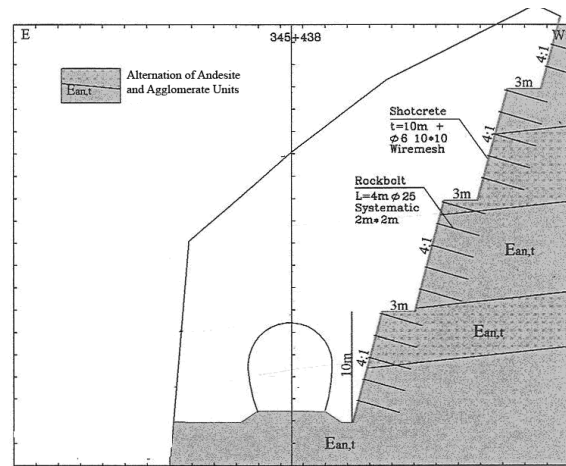


Fig. 3. Portal of Ardebil-Mianeh Railway tunnel chosen as the critical section [10].

#### 4.1. Model geometry

The Ardebil-Mianeh Railway tunnel section 3 is a horseshoe-shape tunnel with a height of about 8 meters and a width of 6 meters. The computational model as well as the joint sets is shown in Figure 4.

The blocks are usually divided into many triangular-shaped constant-strain finite difference zones in UDEC simulations [11]. In this study, a mesh size of 0.2 m was used. The zone of model around the tunnel is shown in Figure 4.

#### 4.2. Material parameters and constitutive models

##### 4.2.1. Rock mass

The Mohr-Coulomb elasto-plastic model was used to represent the behavior of Andesite and Agglomerate rocks as well as the rock joints. The rock mass and joint parameters associated with the Mohr-Coulomb model are tabulated in Tables 7 and 8. It should be noted that the rock mass parameters have been obtained via Rocklab Software using intact rock characteristics and the joint status.

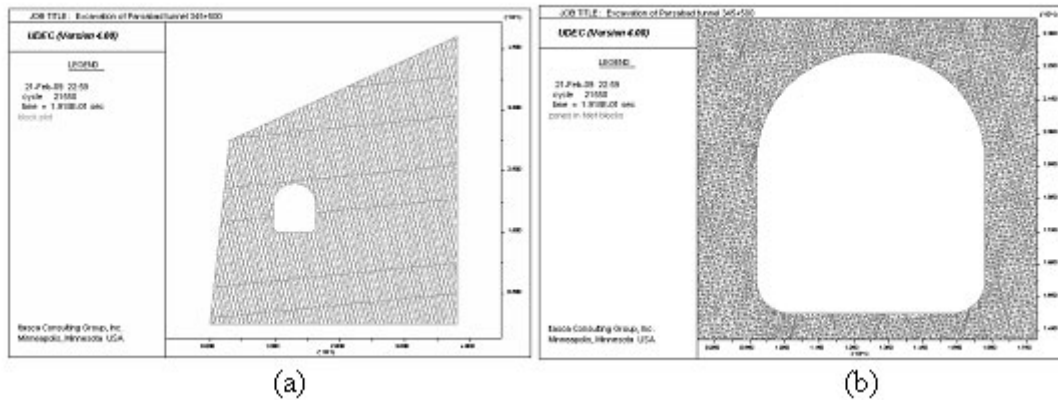


Fig. 4. (a) Geometry of the section chosen for dynamic analysis (b) mesh generation around the tunnel.

Table 7. Andesite and Agglomerate input parameters.

| Rock type   | Density, $\rho$<br>( $\text{kg/m}^3$ ) | Elastic modulus E<br>(GPa) | Bulk modulus, K<br>(GPa) | Shear modulus, G<br>(GPa) | Cohesion, C<br>(MPa) | Friction angle, $\Phi$<br>(Degree) | Tensile strength<br>(MPa) |
|-------------|--|----------------------------|--------------------------|---------------------------|----------------------|------------------------------------|---------------------------|
| Andesite    | 2500                                   | 61.4                       | 40.9                     | 24.5                      | 6                    | 45                                 | 15                        |
| Agglomerate | 2500                                   | 24                         | 16                       | 9.6                       | 2                    | 38                                 | 4.5                       |

Table 8. Rock joint model parameters.

| Joint property  | Cohesion, C<br>(MPa) | Friction angle, $\Phi$<br>(Degree) | Normal stiffness, $K_n$<br>(GPa) | Shear stiffness, $K_s$<br>(GPa) | Tensile strength<br>(MPa) |
|-----------------|----------------------|------------------------------------|----------------------------------|---------------------------------|---------------------------|
| Main joint sets | 0.2                  | 35                                 | 10                               | 4                               | 0.2                       |
| B edding        | 50                   | –                                  | 10                               | 4                               | 10                        |

#### 4.2.2. Tunnel lining

The tunnel lining consists of a 0.3 m thick reinforced concrete. The lining was also assigned with the Mohr-Coulomb elasto-plastic model. The corresponding parameters are shown in Table 9.

#### 4.3. Boundary conditions

In dynamic analysis, the boundary of the model may cause the reflection of the wave that

is propagating outward and decreases the accuracy of the results [19]. For this case, the viscous boundary developed by Lysmer and Kuhlemeyer (1969) [11] was used in the modeling process.

#### 4.4. Mechanical damping

UDEC uses two different forms of damping, local damping and Rayleigh damping, in order to solve the static and the dynamic problems. The former is mainly used in the static solutions,

Table 9. Lining parameters used in UDEC model.

| Concrete property | Density, $\rho$<br>( $\text{kg/m}^3$ ) | Elastic modulus, E<br>(GPa) | Poisson' ratio | Compressive strength, $\sigma_{ci}$<br>(MPa) | Tensile strength<br>(MPa) |
|-------------------|--|-----------------------------|----------------|--|---------------------------|
|                   | 2500                                   | 21                          | 0.25           | 24   | 2.4                       |

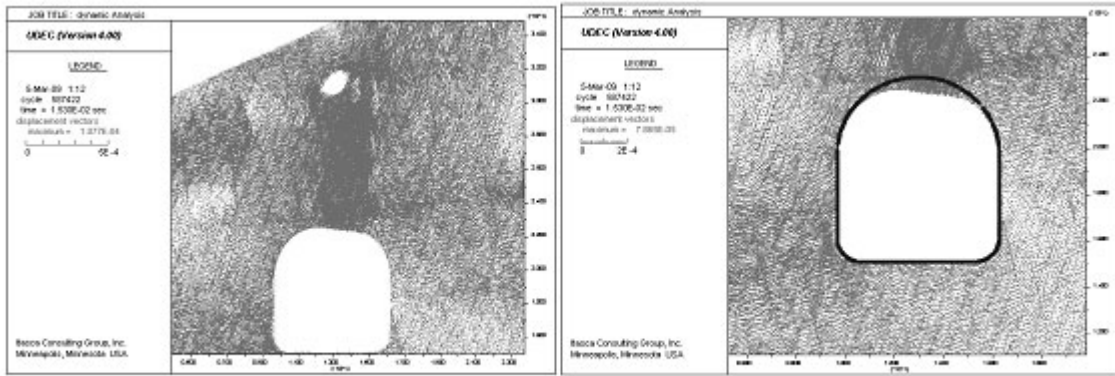


Fig. 5. (a) Displacement field observed in the model, (b) magnified displacement observed around the tunnel.

while the latter is specified for the dynamic problems.

Rayleigh damping is specified in UDEC with the parameters  $f_{min}$  (natural frequency) in Hertz and  $\xi_{min}$  (damping ratio) [11]. The natural frequency, applied in our UDEC modeling, was calculated using the vertical displacement-time curve for a single block contacting on a rigid base with gravity suddenly applied. Thus, a value of 55 Hertz was derived. The theoretical period of oscillation could be derived from the formula given below [11]:

$$frequency = \frac{1}{2\pi} \left( \frac{kl}{m} \right)^{\frac{1}{2}} = 70 \text{ cycles/sec} \quad (9)$$

Where,  $l$  = joint length (15 m, in this case);  
 $k$  = joint stiffness (4 GPa/m); and  
 $m$  = mass of upper block (281,250 kg).

This theoretical formula gives a natural frequency of 70 Hertz.

Finally, we applied the value of 60 Hertz, as the natural frequency, in our dynamic analysis.

According to ITASCA (2004) for geological materials, damping ratio commonly falls in the range of 2 to 5%. Thus, considering a jointed rock medium, an initial value of 3% was used in the current study.

#### 4.5. Modeling results

As the explosion occurs, the rock medium redistributes the blast pressure. Because of the presence of joints, the blast loading could not be

symmetrical throughout the model (Figure 5).

The results indicate that the maximum displacement happens at the tunnel crown. They, also, revealed that the axial force increases from 1.128 tons (in compression) to 2.04 tons (in tension). This gives an increase of 80% in axial force. The maximum bending moment also increased dramatically from 5.55e-2 Ton-m to 2.09e-1 Ton-m (i.e. an increase of 280%).

The variation of maximum axial force and bending moment through-out the dynamic analysis is shown in Figures 6 and 7, respectively.

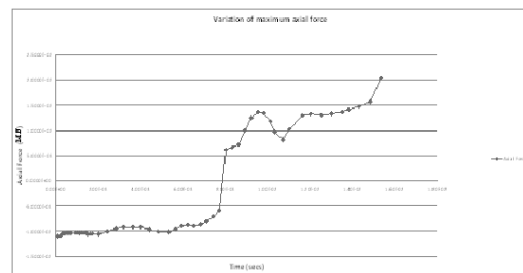


Fig. 6. Variation of maximum axial force through-out the dynamic analysis

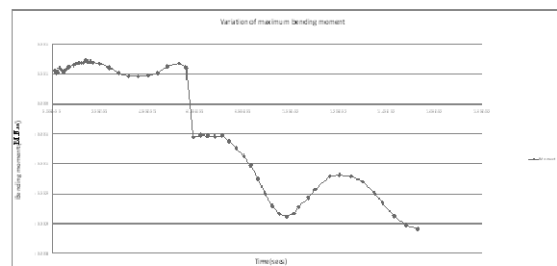


Fig. 7. Variation of maximum bending moment through-out the dynamic analysis

## 5. Conclusion

In this paper, the dynamic response of a tunnel located in a jointed rock mass against projectile impact, is simulated by UDEC. Projectile effects such as penetration, crater forming and wave propagation as well as the discontinuity effect caused by the rock media have been studied. The results show that the tunnel lining is stable under explosion loading but undergoes a considerable increase in axial force and bending moment (an increase of 80% in maximum axial force and an increase of 280% in maximum bending moment). The results also reveal that the axial force goes from compression to tension which should be taken into account for the lining design. The maximum displacement occurs in the tunnel crown which is in accordance with macroscopic investigation on tunnels after explosion in similar cases [20]. The results show that UDEC can be used effectively to simulate the dynamic response of tunnels located in jointed rock media.

## References

- [1] Gui M.W., Chien M.C (2006), "Blast resistant analysis for a tunnel passing beneath Taipei Shongsan airport – a parametric study", *Geotechnical and Geological Engineering*, Vol. 24, 227-248.
- [2] Ma G.W., Hao H., Zhou Y.X. (1998), "Modeling of wave propagation induced by underground explosion", *Computer Geotech. J.*, Vol. 22 (3/4), 283-303.
- [3] Chen S.G., Zhao J. (1998), "A study of UDEC modeling for blast wave propagation in jointed rock masses", *Int. J. Rock Mech. Min. Sci.*, Vol. 35, No.1, 93-99.
- [4] Fan S.C., Jiao Y.Y., Zhao J. (2004), "On modelling of incident boundary for wave propagation in jointed rock masses using discrete element method", *Computers and Geotechnics*, Vol. 31, 57-66.
- [5] Morris J.P., Rubin M.B., Blair S.C., Glenn L.A., Heuze F.E. (2004), "Simulations of underground structures subjected to dynamic loading using the distinct element method", *Engineering computations*, Vol. 21, pp. 384-408.
- [6] Lu Y. (2005), "Underground blast induced ground shock and its modeling using artificial neural network", *J. Computers and Geotechnics*, Vol. 32, 164-178.
- [7] Heuze F.E., Morris J.P. (2006), "Insights into ground shock in jointed rocks and the response of structures there-in", *Int. J. Rock Mech. & Mining Sci.*, Vol. 44, 647-676.
- [8] Jiao Y.Y., Zhang X.L., Zhao J., Q.S. Liu Q.S. (2007), "Viscous boundary of DDA for modeling stress wave propagation in jointed rock", *Int. J. Rock Mech. & Mining Sci.*, 44, 1070-1076
- [9] Wang Z., Li Y., Wang J.G. (2008), "Numerical analysis of blast-induced wave propagation and spalling damage in a rock plate", *Int. J. Rock Mech. Min. Sci.*, Vol. 45, 600-608.
- [10] Iran Ministry of Road and Transportation, Technical report 13-02-348, Parsabad-Ardebil-Nianeh Railway, Second phase study of tunnels.
- [11] ITASCA Consulting Group Inc. (2004), UDEC: Universal Distinct Element Code User's Manual, Version 4.0.
- [12] Department of the US Army Technical Manual TM 5-855-1, "Fundamentals of Protective Design for Conventional Weapons", 1986.
- [13] Bulson P.S., "Explosive loading of engineering structures", E & FN Spon press, 1997.
- [14] Bangash M.Y.H., "Shock, impact and explosion- structural analysis and design", Springer, 2009.
- [15] Ngo T., Mendis P., Gupta A., Ramsay J. (2007), "Blast loading and blast effects on structures – An overview", *EJSE special issue: loading on structures*.



- [16] Jiao Y.Y., Zaho J., Caio J.G. (2003), "Consideration for 2-D and 3-D modelling of shock wave propagation in jointed rock masses", ISRM 2003 – Technology roadmap for rock mechanics, South Africa Institute of Mining and Metallurgy.
- [17] Dowding C.H., Belytschko T.B., Yen H.J. (1983), "Dynamic computational analysis of openings in jointed rock", J. Geotech. Eng., ASCE, Vol. 109, 1551-1566.
- [18] Cundall P.A. (1980), "UDEC- a generalized distinct element program for modelling jointed rock. Peter Cundall Associates, Report PCAR-1-80, U.S. Army, European Research office, London.
- [19] Hart R.D. (1992), "An introduction to distinct element modeling for rock engineering. In comprehensive rock engineering, Vol. 2, ed. J.A. Hudson, pp. 245-261.
- [20] Liu Y.Q., Li H.B., Li J.R., Zhou Q.C. (2004), "UDEC simulation for dynamic response of a rock slope subject to explosions", Int. J. Rock Mech. Min. Sci., Vol. 41, No. 3.
- [21] Hoek E., Kaiser P. K., Bawden W. F., "Support of underground excavations in hard rock", A. A. Balkema/Rotterdam/Brookfield, 1998.
- [22] Cundall P.A., Hart R.D. (1993), "Numerical modelling of discontinues", comprehensive Rock Engineering: Principles, Practices, & Projects, Vol. 2, Hudson (ed.), Pergamon Press.
- [23] Gran J.K., Senseny P.E., Groethe M.A., Chitty D., Trulio J. (1998), "Dynamic response of an opening in jointed rock", Int. J. of Rock Mech. & Mining Sci., Vol. 35(8), 1021-1035.